Membrane cholesterol, lateral mobility, and the phosphatidylinositol 4,5-bisphosphate-dependent organization of cell actin

Jeanne Kwik*†, Sarah Boyle*, David Fooksman*, Leonid Margolis*‡, Michael P. Sheetz§, and Michael Edidin*¶

*Biology Department, The Johns Hopkins University, 3400 North Charles Street, Baltimore, MD 21218; and §Department of Biological Sciences, P.O. Box 2408, Columbia University, 1212 Amsterdam Avenue, New York, NY 10027

Communicated by Joseph G. Gall, Carnegie Institution of Washington, Baltimore, MD, September 23, 2003 (received for review December 9, 2002)

Responses to cholesterol depletion are often taken as evidence of a role for lipid rafts in cell function. Here, we show that depletion of cell cholesterol has global effects on cell and plasma membrane architecture and function. The lateral mobility of membrane proteins is reduced when cell cholesterol is chronically or acutely depleted. The change in mobility is a consequence of the reorganization of the cell actin. Binding of a GFP-tagged pleckstrin homology domain specific for phosphatidylinositol 4,5-bisphosphate [PI(4,5)P2] to the plasma membrane is reduced after cholesterol depletion. This result implies that the reorganization of cytoskeleton depends on the loss or redistribution of plasma membrane PI(4,5)P2. Consistent with this observation, agents that sequester plasma membrane PI(4,5)P2 mimic the effects of cholesterol depletion on actin organization and on lateral mobility.

There is a growing consensus that cell surface membranes are patchworks of domains, local concentrations of membrane proteins, and lipids quite different from the average for an entire membrane (1). Cholesterol is important in organizing some types of domains, usually termed lipid rafts (2, 3). These lipid rafts are thought to be required for cell functions, including directed mobility and capping of membrane proteins, receptor-mediated signaling, entry and exit of pathogens and membrane trafficking (reviewed in ref. 4). Lipid rafts are dispersed when cell cholesterol is extracted (3). Hence, an effect of cholesterol depletion on a particular function is usually assumed to show that lipid rafts are required for this function (5–11). This assumption neglects the way in which the effects of cholesterol depletion ramify beyond local membrane environments and so have global effects on membrane and cell properties.

Our starting point for considering global effects of cholesterol depletion is recent work showing that the key regulatory phospholipid, phosphatidylinositol 4,5-bisphosphate [PI(4,5)P2] is concentrated in cholesterol-dependent domains in proximity to concentrations of F actin, and other components of membrane trafficking (12–16). The localization of PI(4,5)P2 is consistent with its regulated involvement in a wide variety of cell functions (17), particularly regulation of the cytoskeleton (18). Availability of PI(4,5)P2 modulates the cytoskeleton/membrane interaction (19), the stability of cortical actin, and the turnover of cytoplasmic stress fibers (20).

Here, we connect the requirement for cholesterol in organizing plasma membrane PI(4,5)P2 with the role of PI(4,5)P2 in organizing the cytoskeleton. We found that the lateral mobility of plasma membrane proteins was restricted after cholesterol depletion. This effect was reversed by cytochalasin D and was paralleled by changes in organization and turnover of cell actin. The level of PI(4,5)P2 in the plasma membrane was reduced after cholesterol depletion, and the effects of cholesterol depletion were mimicked by sequestering plasma membrane PI(4,5)P2. Thus, cholesterol depletion reduced lateral mobility of membrane proteins because it disrupted the highly regulated interactions of PI(4,5)P2 with molecules controlling the state and organization of the actin cytoskeleton. Because lateral mobility is required for many membrane functions, for example, ligand-induced receptor aggregation and endocytosis, it seems that changes in membrane cholesterol levels can affect cell functions that are themselves independent of lipid rafts.

Methods

Cell Culture and Cholesterol Depletion. Normal human skin fibroblasts, strain 5659, from the NIGMS Human Genetic Cell Repository, Coriell Institute (Camden, NJ) were cultured in Dulbecco's modified Eagle's medium (GIBCO/Invitrogen) supplemented with 10% FBS (Intergen, Purchase, NY), 0.2 mM nonessential amino acids, and 2× vitamins (Invitrogen). JY cells, Epstein–Barr virus-transformed B-lymphoblasts (21) were cultured in RPMI medium 1640 (Invitrogen) supplemented with 10% FBS and 2 mM glutamine.

Fibroblasts and lymphoblasts were chronically depleted of cholesterol by culture in McCoy's medium (Invitrogen) supplemented with 10% lipoprotein-deficient FBS (Intracel, Frederick, MD), instead of with 10% complete FBS. In some experiments, the depletion medium was supplemented with human low-density lipoprotein (LDL, CalBiochem). Fibroblasts were acutely depleted of cholesterol by incubation with 5–10 mM methyl-β-cyclodextrin (MCD, Sigma) for 15–30 min at 37°C in complete medium. MCD was toxic for JY lymphoblasts so these cells were acutely depleted of cholesterol by treatment with 0.5 units of cholesterol oxidase (C8273, Sigma) in complete medium at 37°C for 1 h.

Sequestering PI(4,5)P2 and Expression of Pleckstrin Homology (PH)-GFP. Two methods were used to sequester membrane PI(4,5)P2. In the first, fibroblasts were cultured overnight in medium 0.01 M in neomycin sulfate (Sigma) (22). Washing, labeling, and mounting solutions also contained neomycin. In the second, cells were transfected with a plasmid expressing a GFP-tagged PH domain from phospholipase C-δ (23) by electroporation. After 24–48 h, approximately half the cells were GFP positive. At this point, they were used for the experiments.

Fluorescence Photobleaching and Recovery (FPR) Measurements of Lateral Diffusion. For lateral diffusion measurements, cells were labeled with Cy3 (Amersham Pharmacia)-Fab of a monoclonal antibody, KE2, specific for class I MHC molecules (24). In our standard method, an attenuated laser beam is focused through a ×63 objective to give a spot 0.6- to 0.8-μm radius focused on

Abbreviations: PI(4,5)P2, phosphatidylinositol 4,5-bisphosphate; LDL, low-density lipoprotein; MCD, methyl-β-cyclodextrin; PH, pleckstrin homology.

†Present address: Department of Health and Policy Management, Bloomberg School of Public Health, The Johns Hopkins University, 111 Market Street, Suite 830, Baltimore, MD 21205.

‡Present address: National Institute of Child Health and Human Development, National Institutes of Health, Bethesda, MD 20892.

¶To whom correspondence should be addressed. E-mail: edidin@jhu.edu.

www.pnas.org/cgi/doi/10.1073/pnas.2336102100

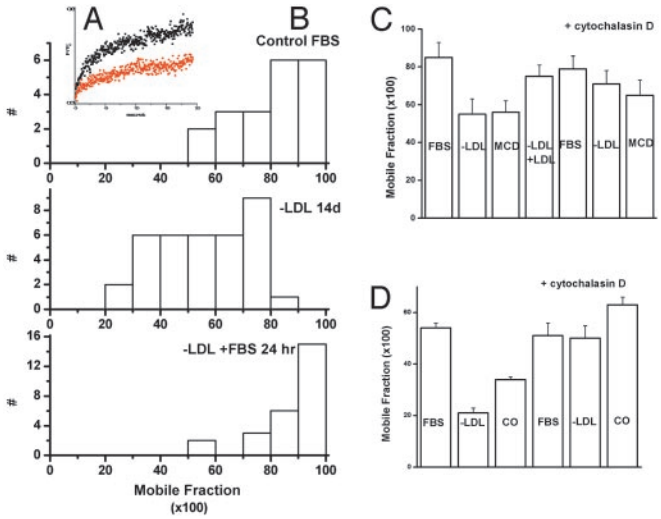

Fig. 1. Cholesterol depletion reduces the lateral mobility of HLA molecules of fibroblasts and lymphoblasts. This reduction is reversed by cytochalasin D. (*A*) Shown is fluorescence recovery after photobleaching of Fab-labeled class I MHC molecules in control 5659c skin fibroblasts (black) and in cells grown in medium lacking LDL (red). Computer fits to these recovery curves estimated maximum recovery as 65–70% for control cells and 30–35% for cells grown without LDL. (*B*) The mobile fractions of class I HLA molecules on fibroblasts grown in control medium (10% FCS, *Top*), medium lacking LDL (*Middle*), or returned to control medium for 24 h after growth for 2 weeks in medium lacking LDL (*Bottom*). The distribution of mobile fractions is shifted to lower mobility after cholesterol depletion but seems similar to the control when cholesterol-depleted cells are cultured in control medium for 24 h. (*C*) The average mobile fraction of class I HLA molecules on 5659c skin fibroblasts either grown without LDL for 10–14 days (−LDL) or acutely depleted of cholesterol by treatment with MCD. Mobile fractions are also shown for cells grown in LDL medium reconstituted with purified LDL (−LDL/+LDL) and for cells treated with cytochalasin D (5 μg/ml) for 30 min. (*D*) The average mobile fraction of class I HLA molecules on JY lymphoblasts either grown without LDL for 10–14 days (−LDL) or acutely depleted of cholesterol by treatment with cholesterol oxidase (0.5 units/ml). Mobile fractions are also shown for cells treated with cytochalasin D (5 μg/ml) for 30 min.

the labeled cell surface. After recording fluorescence from the spot, a fraction of these molecules is bleached by a brief pulse at full laser power. Recovery of the fluorescence in the bleached spot is followed with the attenuated beam. If all molecules are mobile, fluorescence recovers to the level measured before bleaching. The ratio of observed recovery to the initial fluorescence yields the mobile fraction of labeled molecules. For measurements after transfection with PH-GFP, cells were selected for moderate GFP fluorescence by using arc lamp illumination; then, filters were switched to Cy3 for FPR.

Imaging Distribution of PH-GFP Fluorescence. After transfection with PH-GFP, fibroblasts were plated onto 40-mm round coverslips for mounting in a temperature-controlled chamber (Bioptech FCS2, Bioptechs, Butler, PA). Cells were imaged on a Zeiss LSM510 confocal microscope while maintained at 37°C in medium plus 5% lipid-depleted FCS. After collecting image stacks for a set of cells, the medium was changed to one containing 10 mM MCD, and the cells were maintained on the microscope stage for 30 min. The cells were then imaged again. Typically, maximum fluorescence was 20% lower in the second set of images than in the first set. After selecting one section from each of the control and MCD image stacks, the intensity distribution was determined by using the profile tool of the microscope software. In other experiments, involving long-term depletion of cell cholesterol, control and cholesterol-depleted cells were transfected with PH-GFP and 2 days later fixed, and

Fig. 2. Laser trapping of HLA molecules labeled with 40-nm beads. (*A*) HLA I molecules labeled with antibody-coated 40-nm gold beads meet an obstacle as they are dragged along the surface of control fibroblasts. The bead is dragged a little over 1 μm from its initial position, marked by an asterisk (*Left*). In *Center*, it meets an obstacle (at a point marked by the arrowhead) and leaves the trap. Half a second later, the bead is still close to the point where it left the trap. (Bar = 2 μm.) (*B*) HLA I molecules labeled with antibody-coated 40-nm gold beads meet an obstacle as they are dragged along the surface of cholesterol-depleted fibroblasts cultured without LDL for 10–14 days. (*Left*) Initial position of the bead, marked by an arrow. (*Center*) Position of the bead when it meets an obstacle. (*Right*) Shown 0.1 s later, the bead has recoiled in the opposite direction to a point near its starting point.

the intensity distributions across cells were imaged in a DeltaVision (Applied Precision, Issaquah, WA) deconvolution microscope.

Laser Trapping of HLA Molecules Labeled with Antibody-Coated Beads. The laser trap for measuring the movement of labeled molecules in the plane of the cell membrane and the preparation of the labeling beads are described in earlier work from our laboratories (25). Cells transfected with PH-GFP were identified by epifluorescence before trapping. Labeling cells for pulling tethers normal to the membrane, and the trap used to pull these tethers, are described in ref. 19.

Preparation of Triton Cytoskeletons. Triton-extracted cytoskeletons were prepared from 5659c fibroblasts following the protocol of ref. 26. Briefly, cells grown on glass coverslips for 2 days were washed and permeabilized with 0.25% Triton X-100 plus 2% BSA plus protease inhibitors (Protease Inhibitor Mixture, Roche Applied Sciences, Framingham, MA) in isotonic Ca^{2+}-free Hepes-buffered NaCl at 0°C. The permeabilized cells were washed in the isotonic saline, brought to 37°C, and incubated for 10 min at 37°C with a cytoplasmic extract of 293T cells that had been transfected with GFP-actin 2 days earlier. Total protein

Table 1. Frequency of Brownian movements vs. elastic recoil after trapped MHC I molecules meet a barrier and leave the trap

Treatment	No. showing Brownian motion	No. showing elastic recoil	% elastic recoil
Control (FBS)	63	5	7
−LDL	21	26	55
−LDL + cytochalasin D*	7	2	22
+MCD†	9	28	76
+PH-GFP‡	0	15	100

*Cells were treated with 2 ug/ml cytochalasin D for 3 min at room temperature and 20 min at 31°C before trapping. Most cells were too rounded to allow imaging the beads.
†Cells were treated with 10 mM MCD for 20–30 min before trapping.
‡Cells were transiently transfected with the PH domain of phospholipase C-δ, tagged with GFP (PH-GFP). Bright cells were selected for trap measurements by using the arc lamp on the trap microscope.

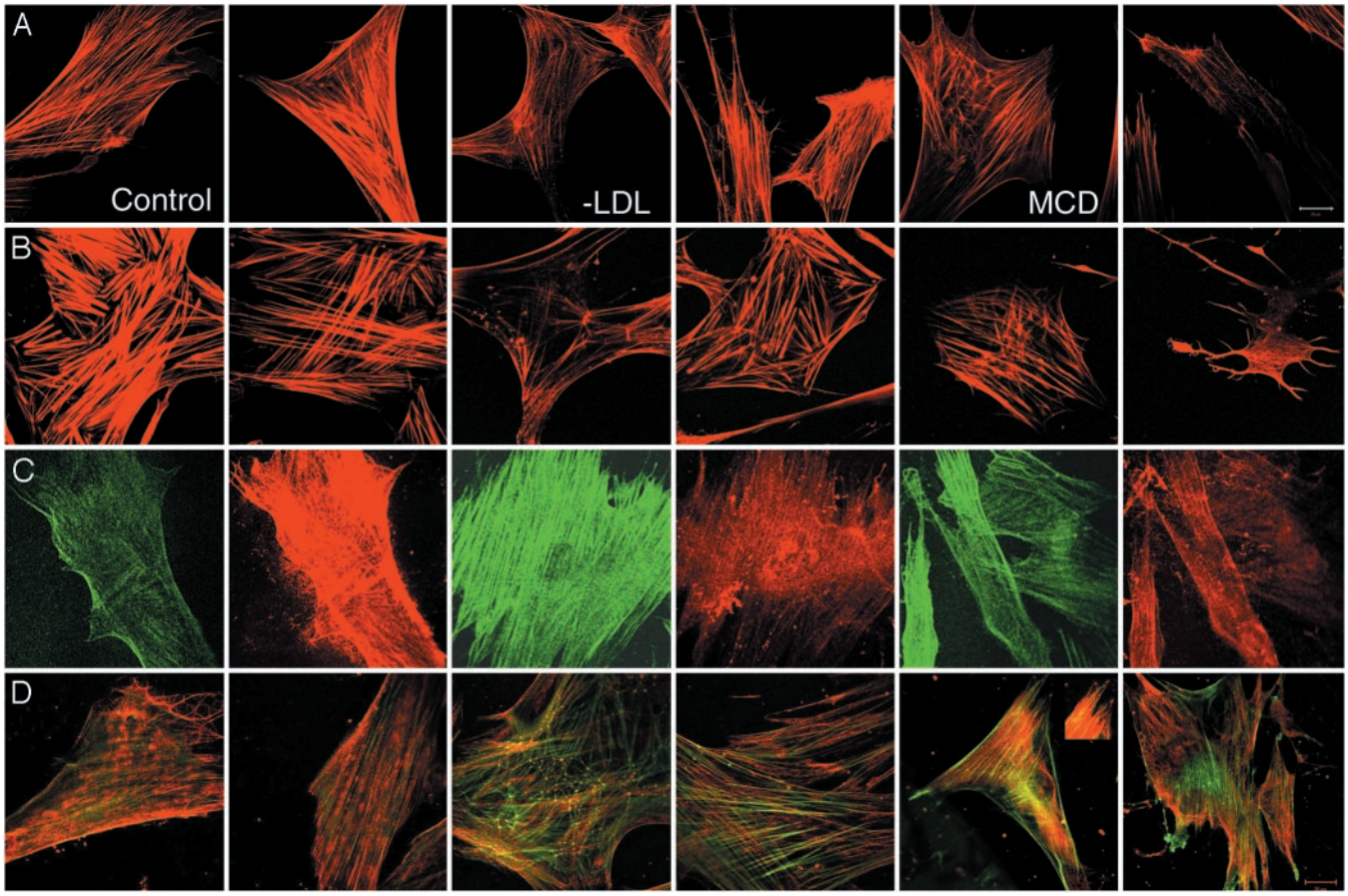

Fig. 3. Cholesterol depletion and organization of the actin cytoskeleton. (*A*) From left to right, two examples each of phalloidin labeling of F-actin in control fibroblasts, fibroblasts grown without LDL for 10–14 days, and fibroblast cells incubated with 5 μM MCD for 15 min at 37°C. Labeled stress fibers are more abundant and apparently thicker in control cells than in cholesterol-depleted cells. (*B*) From left to right, two examples each of phalloidin labeling of F-actin in Triton cytoskeletons prepared from control fibroblasts, fibroblasts grown without LDL for 10–14 days, and fibroblast cells incubated with 10 μM MCD for 30 min at 37°C. Labeled stress fibers are more abundant and apparently thicker in control cells than in cholesterol-depleted cells. Also, radial foci of phalloidin labeling can be seen cholesterol-depleted, but not in control cells. (*C*) From left to right, incorporation of GFP-actin (green) in, and labeling with anti-gelsolin mAb (red) of Triton cytoskeletons prepared from control fibroblasts, fibroblasts grown without LDL for 10–14 days, and fibroblast cells incubated with 10 μM MCD for 30 min at 37°C. The microscope gain was set as constant for all images. Hence, the dimmer green fluorescence and brighter red fluorescence of control cytoskeletons compared with cytoskeletons from cholesterol-depleted cells indicates that there is lower turnover of stress fibers and a higher level of bound gelsolin in the controls than in the cytoskeletons from cholesterol-depleted cells. (*D*) From left to right, two examples each of incorporation of GFP-actin (green) in, and labeling with anti-α-actinin mAb (red) of Triton cytoskeletons prepared from control fibroblasts, fibroblasts grown without LDL for 10–14 days, and fibroblast cells incubated with 10 μM MCD for 30 min at 37°C. The microscope gain used to image controls had to be reduced to yield the images of the second, third, fourth, and sixth panels. The *Inset* of the fifth panel shows a portion of the cell in this panel; imaged with the same gain as controls, it is shown in the fifth panel. (Scale bars = 20 μm.)

concentration of the extract was 5 mg/ml, and ATP was added to a final concentration of 0.5 mM. After incorporating GFP-actin, the cytoskeletons were either fixed in 4% paraformaldehyde (PFA) or were washed and incubated further with monoclonal anti-gelsolin (Sigma G4896) or anti-α-spectrin (Sigma A5044) antibodies followed by Cy5-conjugated goat anti-mouse Ig (Jackson ImmunoResearch). Double-labeled cytoskeletons were also fixed in 4% PFA.

Assay of Cell PI(4,5)P2. Levels of PI(4,5)P2 in cell lipid extracts were assayed by using a commercial binding protein assay (Amersham Pharmacia Biosciences), based on the method of ref. 27. Briefly, PI(4,5)P2 was hydrolyzed to D-myo-inositol 1,4,5-trisphosphate (IP3), and the IP3 was assayed in terms of competition for binding with standard [^{3}H]IP3.

Results and Discussion

We measured the lateral diffusion of typical type 1 transmembrane proteins, of human class I HLA molecules, and of lymphoblasts and fibroblasts. Cholesterol was chronically depleted by growing cells in LDL-deficient medium for 10–14 days, or was acutely depleted by treating cells with cholesterol oxidase (lymphoblasts) or MCD (fibroblasts). All these treatments lowered cell cholesterol to 50–60% of control levels (data not shown). They also decreased the mobile fraction of HLA molecules on the time scale (10s of s) of a fluorescence photobleaching and recovery measurement (Fig. 1). Similar effects were found on the lateral diffusion of the epidermal growth factor receptor after cholesterol depletion (data not shown).

Mobility was not restored by a 3- to 12-h incubation in cholesterol-containing medium (LDL-depleted medium supplemented with LDL, or medium with complete serum) even though cell cholesterol levels were 1.5–2 times those of controls (presumably because cholesterol-depleted cells up-regulate LDL receptors) but rather returned to control levels by 24 h (Fig. 1*B Bottom*) when cell cholesterol levels were the same as in controls. However, brief (30-min) treatment of cholesterol-depleted cells with cytochalasin D, depolymerizing F actin, returned the im-

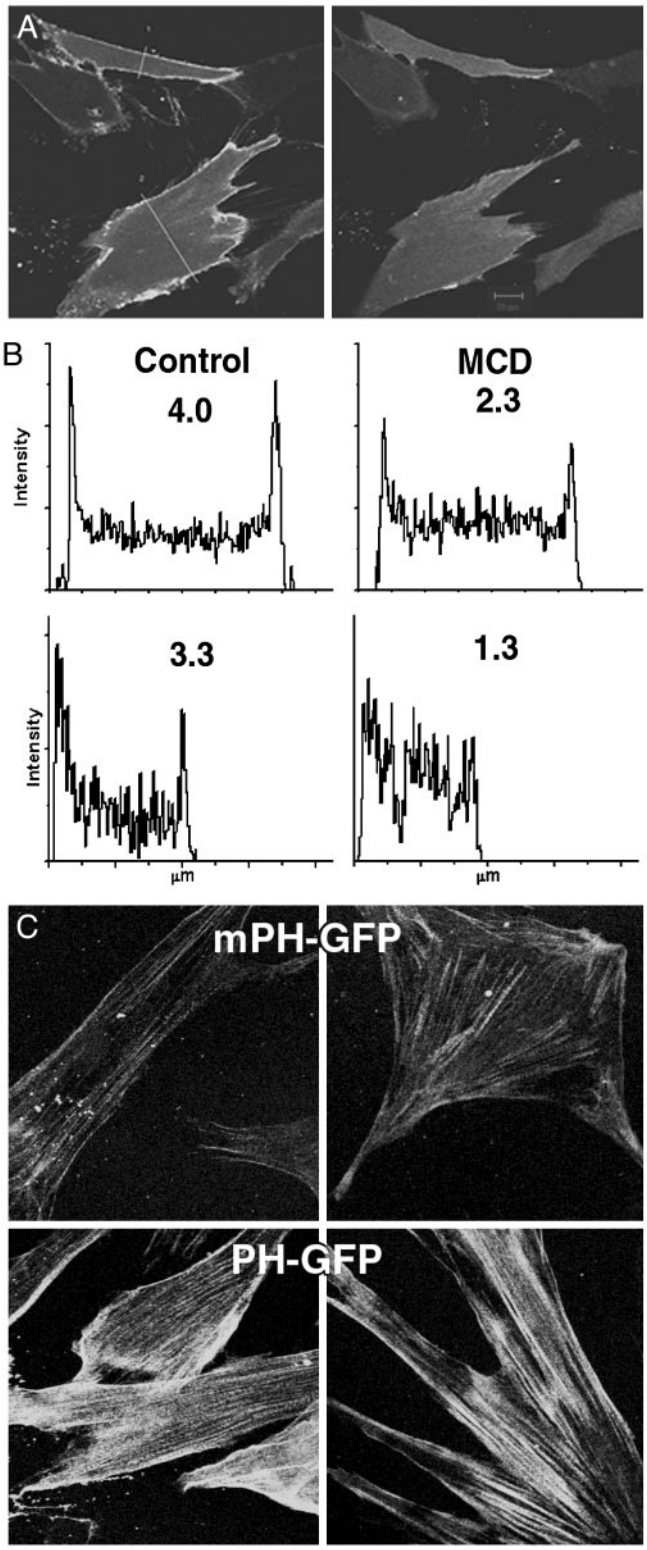

Fig. 4. Cholesterol depletion, distribution of PI(4,5)P2 measured in terms of distribution of PH-GFP, and effects of PH-GFP expression on actin cytoskeleton. (*A*) Confocal microscope sections of cells expressing PH-GFP. Cells were cultured in a Bioptech chamber and imaged in medium at 37°C before cholesterol depletion (*Left*) and after incubation with 10 mM MCD for 20 min (*Right*). (*B*) The distribution of GFP fluorescence across the cells (marked by white lines in *A*) is shown before cholesterol depletion (*Left*) and after cholesterol depletion with MCD (*Right*). It can be seen that the ratio of membrane-bound to cytoplasmic GFP fluorescence shifts to the cytoplasm after cholesterol depletion. (*C*) Incorporation of GFP-actin by Triton cytoskeletons from cells transfected with a mutant PH domain that does not bind PI(4,5)P2 (*Upper*) or by cytoskeletons from cells transfected with PH-GFP, which does bind PI(4,5)P2 (*Lower*). More GFP-actin is incorporated when a PI(4,5)P2-sequestering PH domain is expressed than when the mutant is expressed. (Bar = 20 μm.)

mobile fraction to the level of control cells (Fig. 1 *C* and *D*). Thus cholesterol depletion seemed to stabilize the submembrane skeleton.

Labeling class I molecules on fibroblasts with 40-nm gold beads allowed them to be trapped in a laser trap and dragged across the cell surface (25). When the labeled molecules met an obstacle, they came out of the trap and showed Brownian motion. Fig. 2*A* shows this behavior. A bead attached to HLA molecules is trapped in *Left*. In *Center*, it is dragged a distance of $\approx$1 μm toward the edge of the cell (upper part of the frame). At the end of this movement, it meets an obstacle and comes out of the trap. *Right* shows that, after leaving the trap, the particle remains in the vicinity of the obstacle, far from its starting position, marked by an asterisk. In contrast, in cholesterol-depleted cells, HLA molecules meeting an obstacle and coming out of the trap (Fig. 2*B Center*) snapped back a distance of a micrometer or more, taking a fraction of a second to reach the position where they were first trapped (Fig. 2*B Right*). This result implied that they were anchored to or confined by an elastic element of the cytoskeleton (28). Elastic recoil was rare in control cells (Table 1) but was seen for more than half of the particles trapped on cholesterol-depleted cells. The frequency of elastic recoils was reduced by brief treatment of cholesterol-depleted cells with cytochalasin D (Table 1).

To distinguish between anchoring to the cytoskeleton and confinement by the membrane-associated cytoskeleton, a laser trap was used to pull bead-attached HLA molecules perpendicular to the surface (23). If the HLA molecules were not attached to the cytoskeleton, then the membrane could be pulled off the surface, to create tubes of membrane, or tethers. If they were attached to the cytoskeleton, then tethers could not be formed. Hence, if HLA molecules were more efficiently anchored to the cytoskeleton in cholesterol-depleted cells than in control cells, then they would be more difficult to pull from the surface compared with control cells. Instead we found that tethers were more easily pulled on cholesterol-depleted than on control cells, implying fewer attachments to the cytoskeleton. About 75% of all beads placed on the surface attached to either control or cholesterol-depleted cells. In control cells, between 10% and 25% of these beads could be pulled to yield a membrane tether, even at high (1,110 mW) trap power. In contrast, 60% of beads could be pulled to yield tethers from cholesterol-depleted cell membranes. Therefore, confinement by an elastic membrane skeleton, rather than anchoring to that skeleton, better explains the inhibition of lateral movement and elastic behavior of bead-labeled HLA molecules in cholesterol-depleted cells.

Changes in actin cytoskeleton after cholesterol depletion were also evident as changes in the organization and activity of actin and actin-modifying proteins. Overall, the images suggest that the cytoplasmic actin cytoskeleton is less stable in cholesterol-depleted cells than in controls. Control cells and their Triton cytoskeletons had prominent stress fibers staining with rhodamine phalloidin (Fig. 3 *A* and *B*, first and second panels). There were fewer, thinner stress fibers in LDL-depleted and MβCD-treated cells and in their Triton cytoskeletons. There were also numerous foci of actin polymerization in cholesterol-depleted cells (Fig. 3 *A* and *B*, third through sixth panels). When treated with very high concentrations (10 mM) of MβCD for a relatively long time (30 min), cells developed extensive microspikes that labeled for F-actin (data not shown). Triton cytoskeleton preparations from control cells incorporated less G-actin than cy-

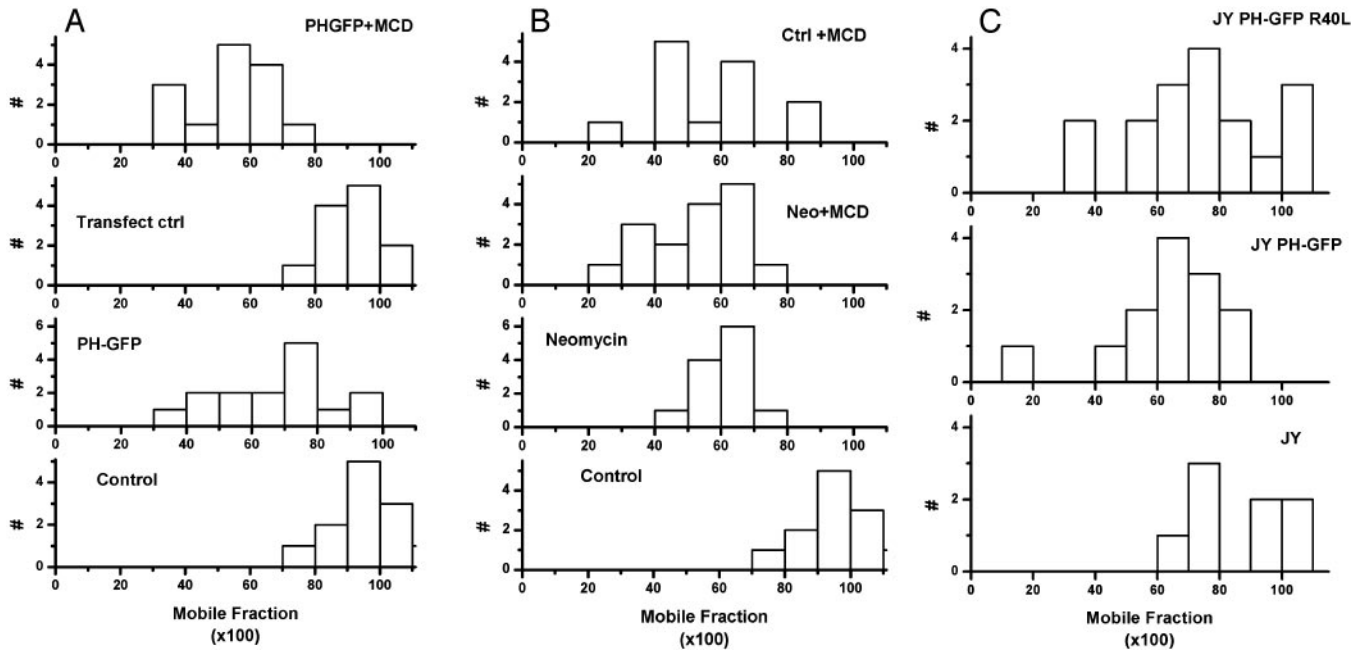

Fig. 5. Effect of sequestering PI(4,5)P2 on lateral mobility of class I HLA molecules. (*A*) Distribution of lateral mobility of HLA molecules in fibroblasts cultured overnight in neomycin compared with that in control cells or cells acutely depleted of cholesterol with MCD. The distribution of mobile fractions in cells treated with both neomycin and MCD is also shown. (*B*) Distribution of lateral mobility of HLA molecules in fibroblasts transfected with low levels of PH-GFP compared with that in cells not expressing the PH domain after transfection and to the distribution in PH-GFP-expressing cells also treated with MCD. The mutant GFP-PH domain used as a control for lymphoblasts (5C) could not be used for fibroblasts because it was always expressed at very high levels and its fluorescence bled through into the fluorescence photobleaching and recovery channel of the microscope, creating an artifact of fluorescence recovery. (*C*) Distribution of lateral mobility of HLA molecules in JY B-lymphoblasts transfected with low levels of PH-GFP compared with the distribution of values in cells expressing a mutant PH domain that does not bind PI(4,5)P2.

toskeletons of cholesterol-depleted cells and contained relatively higher levels of gelsolin, much of which was associated with stress fibers (29). This result is evident from the relative intensities of green (GFP-G actin) and red (anti-gelsolin antibody) fluorescence in the images of Fig. 3*C*. Levels of α-actinin were higher in the depleted cells than in controls (compare the intensity of the *Inset* of Fig. 3*D*, fifth panel with the rest of the figure). And its distribution was somewhat different. In controls it localized in small protrusions, along stress fibers in a characteristic dot pattern as reported (e.g., ref. 30), and in patches that may represent focal adhesions (Fig. 3*D*, first and second panels). These patches were also seen in cholesterol-depleted cells. In addition α-actinin was also present in a reticular network close to the surface and, as well, in the foci of actin polymerization (Fig. 3*D*, third through sixth panels).

The changes in actin cytoskeleton that we observed are consistent with changes in the activity of actin-modifying proteins that are regulated by PI(4,5)P2 (18). Cholesterol depletion disrupts organization of PI(4,5)P2 in the plasma membrane (13), and some of the changes in cell morphology that we observed after acute cholesterol depletion, especially the formation of numerous microspikes, are similar to those observed when plasma membrane PI(4,5)P2 is sequestered by so-called GMC proteins (15). The increased stability of the cortical cytoskeleton reflected in our fluorescence photobleaching and recovery and laser trap experiments and the increased turnover of stress fibers in cytoskeletons from cholesterol-depleted cells are also consistent with a loss or redistribution of available PI(4,5)P2 from the plasma membrane (20, 31).

The amount of total cell PI(4,5)P2 changed $<20\%$ after acute or chronic cholesterol depletion (data not shown). However, there was relatively less PI(4,5)P2 in the plasma membrane of cholesterol-depleted cells than in controls. We quantified this change by measuring changes in the distribution of the PH domain of phospholipase C-δ, tagged with GFP (PH-GFP) (23, 32, 33) between plasma membrane and cytoplasm. Fig. 4 illustrates an experiment in which fibroblasts were imaged before and after incubation in 10 mM MCD. Five cells are shown in the confocal micrographs of Fig. 4*A*, and the distribution of PH-GFP fluorescence before and after MCD is shown for two of the cells in Fig. 4*B*. In 48 measurements on 16 different cells, we found that the ratio of GFP fluorescence at the plasma membrane to that in the cytoplasm decreased somewhat $>$2-fold. It averaged 4.5 ± 0.4 SEM for cells before MCD treatment and 1.8 ± 0.3 after MCD treatment. A similar decrease in the ratio of plasma membrane PH-GFP to cytoplasmic PH-GFP was measured when populations of control cells were compared with populations of cells deprived of LDL for 10–12 days (2.4 ± 0.2 SEM for control vs. 1.4 ± 0.1 for LDL depleted), but there was little change in distribution (2.00 ± 0.2) when cells were cultured in depletion medium supplemented with LDL. It seems that level of PI(4,5)P2 available for binding by PH-GFP is higher in the plasma membrane of control cells than in the plasma membrane of cholesterol-deprived cells. The decreased PI(4,5)P2 labeling by PH-GFP correlates with a reorganization of the actin cytoskeleton.

If PI(4,5)P2 regulation of the actin cytoskeleton depends on its local concentration and availability in the plasma membrane, then we expect that sequestering PI(4,5)P2 should have effects similar to cholesterol depletion. The PH-GFP domain that we used as a probe for PI(4,5)P2 localization can also be used to sequester PI(4,5)P2. Triton cytoskeletons prepared from cells expressing PH-GFP incorporated more GFP-G actin into stress fibers than did cytoskeletons from cells expressing a mutant PH-GFP which does not bind PI(4,5)P2 (Fig. 4*C*), just the difference that we observed between cytoskeletons of choles-

terol-depleted and control cells. Laser-trapped HLA molecules on the surface of fibroblasts expressing PH-GFP all showed elastic recoil, rather than Brownian when they met obstacles (Table 1), again the same effect seen in cholesterol-depleted cells. Finally, we found that sequestering PI(4,5)P2 by expressing PH-GFP or by incubating cells with neomycin, which binds and sequesters PI(4,5)P2 (22), decreased the mobile fraction of MHC class I molecules to about the same extent as cholesterol depletion (Fig. 5). There seems to be a lower limit to the modulation of lateral diffusion by cholesterol depletion and dispersion of PI(4,5)P2. The combination of cholesterol depletion and sequestering PI(4,5)P2 had no greater effect on lateral diffusion than either treatment alone (Fig. 5 *B* and *C*). Consistent with this result, cholesterol depletion of lymphoblasts had no effect on the mobile fraction of lymphocyte function-associated antigen (LFA-1) and intercellular adhesion molecule-1 (ICAM-1), molecules that are mostly (≈65%) immobile in control cells (data not shown).

Our data show that regulated PI(4,5)P2 activity is required for regulation of the cell cytoskeleton. Depleting cell cholesterol and decreasing plasma membrane levels of PI(4,5)P2 relative to those in the cytoplasm upset this regulation. This upset results in global, rather than merely local, effects on plasma membrane function, mediated through changes in the actin cytoskeleton. Our results also imply that effects of cholesterol depletion on any given cell function may report requirements for lateral diffusion or aggregation of membrane proteins, rather than reporting direct involvement of lipid rafts in the function studied.

We thank Dr. Tamas Balla, National Institute of Child Health and Human Development, National Institutes of Health, for the PH-GFP plasmid and Dr. Hewang Li for the PI(4,5)P2 assays. Cells were imaged on microscopes of the Integrated Imaging Center, Department of Biology, The Johns Hopkins University. This research was supported by National Institutes of Health Grant AI14584 (to M.E.).

1. Edidin, M. (2001) *Trends Cell Biol*. **11,** 492–496.
2. Simons, K. & Toomre, D. (2000) *Nat. Rev. Mol. Cell Biol*. **1,** 31–39.
3. Brown, D. & London, E. (2000) *J. Biol. Chem*. **275,** 17221–17224.
4. Edidin, M. (2003) *Annu. Rev. Biophys. Biomol. Struct*. **32,** 257–283.
5. Xavier, R. Brennan, T, Li, Q., McCormack, C. & Seed, B. (1998) *Immunity* **8,** 723–732.
6. Kabouridis, P., Janzen, J., Magee, A. L. & Ley, S. C. (2000) *Eur. J. Immunol*. **30,** 954–963.
7. Nguyen, D. & Hildreth, J. E. K. (2000) *J. Virol*. **74,** 3264–3272.
8. Rodal, S. K., Skretting, G., Garred, O., Vilhardt, F., van Deurs, B & Sandvig, K. (1999) *Mol. Biol. Cell* **10,** 961–974.
9. Subtil, A., Gaidarov, I., Kobylarz, K., Lampson, M. A., Keen, J. H. & McGraw, T. E. (1999) *Proc. Natl. Acad. Sci. USA* **96,** 6775–6780.
10. Pelkmans, L., Puntener & Helenius, A. (2002) *Science* **296,** 535–539.
11. Lang, T., Bruns, D., Wenzel, D., Riedel, D., Holroyd, P., Thiele, C. & Jahn, R. (2001) *EMBO J*. **20,** 2202–2213.
12. Caroni, P. (2001) *EMBO J*. **20,** 4332–4336.
13. Pike, L. J. & Miller, J. M. (1998) *J. Biol. Chem*. **273,** 22298–22304.
14. Sechi, A. S. & Wehland, J. (2000) *J. Cell Sci*. **113,** 3685–3695.
15. Laux, T., Fukami, K., Thelen, M., Golub, T., Frey, D. & Caroni, P. (2000) *J. Cell Biol*. **149,** 1455–1472.
16. Rozelle, A. L., Machesky, L. M., Yamamoto, M., Driessens, M. H., Insall, R. H., Roth, M. G., Luby-Phelps, K., Marriott, G., Hall, A. & Yin, H. L. (2000) *Curr. Biol*. **10,** 311–320.
17. McLaughlin, S. Wang, J., Gambhir A. & Murray D. (2002) *Annu. Rev. Biophys. Biomol. Struct*. **31,** 151–175.
18. Yin, H. L. & Janmey, P. A. (2003) *Annu. Rev. Physiol*. **65,** 761–789.
19. Raucher, D., Stauffer, T., Chen, W., Shen, K., Guo, S., York, J. D., Sheetz, M. P. & Meyer, T. (2000) *Cell* **100,** 221–228.
20. van Rheenen, J. & Jalink, K. (2002) Mol. *Biol. Cell* **13,** 3257–3267.
21. Terhorst, C. (1976) *Proc. Natl. Acad. Sci. USA* **73,** 910–914.
22. Arbuzova, A., Martushova, K., Hangyas-Mihalyne, G., Morris, A. J., Ozaki, S., Prestwich, G. D. & McLaughlin, S. (2000) *Biochim. Biophys. Acta* **1464,** 35–48.
23. Varnai, P. & Balla, T. (1998) *J. Cell Biol*. **143,** 501–510.
24. Schreiber, A. B., Schlessinger, J. & Edidin, M. (1984) *J. Cell Biol*. **98,** 725–731.
25. Edidin, M. Kuo, S. C. & Sheetz., M. P. (1991) *Science* **254,** 1379–1382.
26. Sawada, Y. & Sheetz, M. P. (2002) *J. Cell Biol*. **156,** 609–615.
27. Chilvers, E. R., Batty, I. H., Challiss, R. A. J., Barnes, P. J. & Nahorski, S. R. (1991) *Biochem. J*. **275,** 373–379.
28. Suzuki, K. & Sheetz M. P. (2001) *Biophys. J*. **81,** 2181–2189.
29. Chou, J., Stolz, D. B., Burke, N. A., Watkins, S. C. & Wells, A. (2002) *Int. J. Biochem. Cell Biol*. **34,** 776–790.
30. Turnacioglu, K. K., Sanger, J & Sanger J. (1998) *Cell Motil. Cytoskel*. **40,** 59–70.
31. Yamamoto, M., Hilgemann, D. H., Feng, S., Bito, H., Ishihara, H., Shibasaki, Y. & Yin, H. L. (2001) *J. Cell Biol*. **152,** 867–876.
32. Raucher, D. & Sheetz, M. P. (2001) *J. Cell Sci*. **114,** 3759–3766.
33. Balla, T. & Varnai P. (2002) *Science STKE*, stke.sciencemag.org/cgi/content/full/sigtrans;2002/125/pl3.